Coag-Flocculation of Mucuna Seed Coag-Flocculant (MSC) in Coal Washery Effluent (CWE) Using Light Scattering Effects

M. C. Menkiti, and O. D. Onukwuli
Dept. of Chemical Engineering, Nnamdi Azikiwe University, Awka, Nigeria

DOI 10.1002/aic.12665
Published online June 14, 2011 in Wiley Online Library (wileyonlinelibrary.com).

Keywords: coal effluent, coag-flocculation, kinetics, mucuna, coagulation

Introduction

Coag-flocculation behavior of MSC with respect to pH variation in CWE has been investigated at room-temperature using various dosages of unblended MSC. Coag-flocculation parameters such as reaction order, rate constant K_m, period, etc., were determined. Turbidity measurement was carried out using the single angle (90°) standard nephelometric jar test, while MSC production was based on the work of Adebowale and Adebowale. The maximum MSC performance are recorded at $K_m = 8.3334 \times 10^{-3}\text{m}^3/\text{kg.s}$, dosage of 0.15 kg/m^3, pH of 6 and period $\tau_{½} = 1.7339$ s. The minimum efficiency (E) is $> 88\%$, thus, confirming MSC as effective coag-flocculant. Generally, the results obtained are in agreement with previous works. Hence, perikinetics theory holds for coag-flocculation of CWE using MSC at the conditions of the experiment.

Coagulation/flocculation (coag-flocculation) ranks among the most critical unit processes apart from filtration and disinfection. Often, it is the first unit process and crucial for the removal of suspended and dissolved particles (SDP).Conceptually, coag-flocculation is the process of adding substances to waste effluent to make the SDP to bind together (coagulation), and subsequently aggregate into visible flocs (flocculation) that settle out of the water.[1–5] Readily, coag-flocculation has been achieved via inorganic substances such as alum $FeCl_3$, etc. However, the coag-flocculation performances of these aggregating agents are well documented with inadequate attention, given to the study of coag-flocculation behavior of the plant and animal derivatives. To this end, focus here is given to the study of coag-flocculation performance of the plant material, Mucuna bean seed.

Mucuna sloanei is abundant in eastern Nigeria. It is an annual twinning tropical plant with pods containing seed bean, which is the bearer of the active component (proteins) that is processed into mucuna seed coag-flocculant (MSC). The seeds which are edible and nontoxic are high in soluble proteins (20–30%), lipids, fibers, minerals and L-dopa.[6] Previous results from thickening studies with MSC highlight prospects of renewable organic material with possible extensive application in large-scale water treatment technology.[7] This work, therefore, evaluates coag-flocculation performance of MSC under varying MSC dosages and CWE pH using single angle (90°), and simulated multiangle light scattering techniques. Expectedly, the post usage handling and health challenges posed by the inorganic coagulants can be eliminated or minimized.

Theoretical Principles and Model Development

For a uniformly coag-flocculating equilibrium phase with negligible influence of external force[8]

$$\mu_i = \bar{G}_i = \left[\frac{\partial G}{\partial n_i}\right]_{P,T,n} = \text{a constant} \tag{1}$$

and

$$D' = K_B T/B \tag{2}$$

where D' is diffusion coefficient, B is the friction factor, K_B is the Boltzmanns constant, T is the temperature, G is the total Gibbs free energy, n_i is the number of moles of component i, and μ_i is the chemical potential.

Correspondence concerning this article should be addressed to M. C. Menkiti at cmenkiti@yahoo.com.

In a similar phase (assuming monodispersed, no breakup and *bi* particle collision), the rate of successful coag-flocculation collision between particles of sizes i and j to form particle of size k is expressed by[5,9,10]

$$\frac{dn_k}{dt} = \frac{1}{2}\sum_{i+j=k}\beta_{BR}(i,j)n_i n_j - \sum_{i=1}^{\infty}\beta_{BR}(i,k)n_i n_k \tag{3}$$

where β_{BR} (i,j) is Brownian aggregation collision factor for flocculation transport mechanism, and $n_i n_j$ is the particle aggregation concentrations for particles of size i and j, respectively.

Jin,[5] Hunter[8] and Fridkhsberg[11] showed, respectively, that

$$\beta_{BR} = \frac{8}{3}\varepsilon_p\frac{K_B T}{\eta} \tag{4}$$

and

$$K_R = 8\pi a D' \tag{5}$$

where K_R is the Von smoluchowski rate constant for rapid coagulation, α is the particle radius, ϵ_p is the collision efficiency, and η is the viscosity of the fluid.

Equation 5 is simplified to

$$K_R = \frac{4}{3}\frac{K_B T}{\eta} \tag{6}$$

According to Van Zanten and Elimelech,[12] it is shown that

$$K_v = \varepsilon_p K_R \tag{7}$$

where K_v is a constant for α^{th} order aggregation at an early time of the process. Equation 7 can be transformed to

$$K_m = \frac{1}{2}\beta_{BR} \tag{8}$$

where K_m is defined as Menkonu coag-flocculation rate constant accounting for Brownian coag-flocculation transport of destabilized particles at α^{th} order.

For Brownian coag-flocculation[8,9,10]

$$-\frac{dN_t}{dt} = K_m N_t^{\alpha} \tag{9}$$

N_t is the concentration of SDP at time t.

Empirical evidence shows that in real practice: $1 \leq \alpha \leq 2$.[13–17] Graphical representation of linear form of Eq. 9 at $\alpha = 1$ or 2 should give a straight-line graph, and K_m can be measured from the slope of either of the following equations

$$\alpha = 1 : \ln\left(\frac{1}{N}\right) = K_m t - \ln N_0 \tag{10}$$

$$\alpha = 2 : \frac{1}{N} = K_m t + \frac{1}{N_0} \tag{11}$$

Where N_0 is the initial N_t at time $= 0$, and N is N_t at upper time limit > 0.

Equation 11 can be solved to obtain coag-flocculation period $\tau_{1/2}$

$$\tau_{1/2} = {}^{1}/_{(0.5N_0K_m)} \tag{12}$$

For Brownian (perikinetic) aggregation at early stages ($t \leq 30$ min), Eq. 3 can be solved exactly, resulting in the generic expression

$$\frac{N_{m(t)}}{N_0} = \frac{\left[{}^{t}/_{\tau^{1}/_{2}}\right]^{m-1}}{\left[1 + {}^{t}/_{\tau_{1}/_{2}}\right]^{m+1}} \tag{13}$$

where $m = 1$ (singlets), 2 (doublets), and 3 (triplets). Equation 13 is used for the graphical representation of time course particle distribution.

Coag-flocculation w.r.t. multiangle light scattering system at the initial intensity changes with time result in

$$I(q,\mathrm{T}_d) = I(q,0)\left[1 + 2\frac{\sin qd_0}{qd_0}\frac{\mathrm{T}_d}{(1+\mathrm{T}_d)^3} + 2\sum_{m=3}^{\infty}C_m(\mathrm{T}_d)A_m(q)\right] \tag{14}$$

where T_d is the dimensionless time, d_o is the hard core interaction diameter of the primary particle, C_m (T_d) is reduced number concentration of m-fold aggregation, $I(q, T_d)$ is the scattered light intensity, $I(q,0)$ is intensity of light scattered by initially unaggregated suspension, q is the scattering wave vector, and A_m is the form factor for an aggregate consisting of m primary particle.

Differentiating Eq. 14 with respect to time yields

$$\frac{I}{I(q,0)}\left(\frac{dI(q,t)}{dt}\right)_{t\to 0} = \left[\beta_{BR}N_0\frac{0}{qd_0}\right] \tag{15}$$

By plotting the simulated version of Eq. 15, the slope $(\beta_{BR}N_0)$ could be obtained from the graph of $\frac{I}{I(q,0)}\left(\frac{dI(q,t)}{dt}\right)_{t\to 0} Vs \frac{\sin qd_0}{qd_0}$ from where the simulated K_m, named K_S could be determined. A key highlight in this theory development is the presentation of $2K_m = \beta_{BR}$, correlating single and multiangle light scattering models.

Materials and Methods

The sample of mucuna bean seed was sourced from Eke central market, Awka, Nigeria, and processed to MSC based on the work reported by Adebowale and Adebowale.[18] The jar test was conducted based on standard bench-scale nephelometric method (single-angle procedure) for the examination of water and wastewater.[13,19].

Results and Discussion

A summary of the representative values of coag-flocculation functional parameters for 0.15 kg/m^3 MSC dosage at pH 2, 4, 6, 8, 10 as determined in this study is shown in Table 1. Such similar values (not shown) were also determined for

Table 1. Coag-Flocculation Functional Parameters for Varying pH and Constant Dosage of 0.15kg/m^3 MSC

Parameter	pH=2	pH=4	pH=6	pH=8	pH=10
α	2	2	2	2	2
R^2	0.995	0.999	0.830	0.666	0.954
K_m (m^3/kg.s)	3.333×10^{-3}	6.667×10^{-3}	8.333×10^{-3}	1.667×10^{-3}	1.1667×10^{-4}
β_{Br} (m^3/kg.s)	6.667×10^{-3}	13.333×10^{-3}	16.667×10^{-3}	3.333×10^{-3}	2.333×10^{-4}
K_R (m^3/s)	1.418×10^{-17}	1.384×10^{-17}	1.379×10^{-17}	1.284×10^{-17}	1.131×10^{-17}
ε_p (kg^{-1})	4.702×10^{14}	9.631×10^{14}	12.087×10^{14}	2.597×10^{14}	2.062×10^{13}
$\tau_{1/2}(s)$	4.344	2.167	1.734	8.670	123.848
$(SDP)_0^c$ (kg/m^3)	0.500	3.333	0.0943	1.25	16.667
$(Np)_0^c$ (/m^3)	3.011×10^{26}	2.007×10^{27}	5.679×10^{25}	7.528×10^{26}	1.004×10^{28}
$-r$ (Kg/ m^3.s)	3.333×10^{-3} c^2	6.667×10^{-3} c^2	8.333×10^{-3} c^2	1.667×10^{-3}c^2	1.1667×10^{-4}c^2

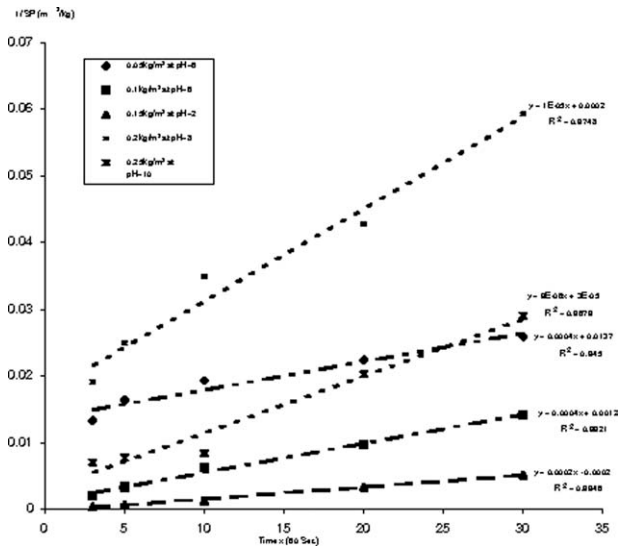

Figure 1. Selected plots of 1/SDP vs. time.

0.05, 0.10, 0.20, and 0.25kh/m^3 MSC dosages at the same pH range.

The accuracy of the fit of the studied model (Eq. 11) with experimental data was determined based on squared linear regression coefficient (R^2). Table 1 indicates that the experimental data (with $R^2 > 0.99$) were significantly described by the linearized form of Eq. 9 (at $\alpha = 2$) expressed as Eq. 11.

K_m is determined from the slope of Eq. 11 on fitting the experimental data on the plot of 1/N or (1/SDP) against time. Representative results are shown in Figure 1. K_m (= 0.5 β_{BR}) as expressed in Eq. 8 shows its least variation between pH of 2 to pH of 6 for all the dosages studied. The optimum K_m (8.333×10^{-3} kg/m^3.s) is obtained at pH of 6 as indicated in the representative Table 1. The value of $\tau_{1/2}$ obtained from Eq. 12 and solved for pH 6 ($\tau_{1/2} = 1.734$ s), lays credence to optimal value of K_m recorded at pH 6. The results displayed in Table 1 show that high K_m corresponds to low $\tau_{1/2}$, a relationship that establishes a strong link among K_m, $\tau_{1/2}$ and rate of aggregation. The optimal $\tau_{1/2}$ (1.734 s) obtained at pH 6 is satisfactory in view of previous works where milliseconds had been reported.[8]

ϵ_p and K_R were obtained from Eqs. 4 and 6, respectively. ϵ_p is obtained when K_R (Eq. 6) is substituted into Eq. 4. Generally, the variation of $K_R = fn\ (T, \eta)$ is minimal, following insignificant changes in the values of temperature and viscosity of the effluent medium. At approximately invariant K_R, ϵ_p relates directly to $2K_m = \beta_{BR}$ (Eq. 8). Thus, high ϵ_p results in high-kinetic energy to overcome the zeta potential. From the theoretical point of view, $\tau_{1/2}$, ϵ_p and K_R are considered as effectiveness factors, understood to be accounting for the coagulation efficiency before flocculation sets in.

K_s (simulated version of K_m) can be determined by plotting the initial normalized intensity change at each scattering angle as a function of its corresponding dimer interference factor, as indicated in Eq. 15. The slope of such a curve is $\beta_{BR}N_0$. The rate constant, K_s is determined from this slope. Representative results are shown in Table 2 and Figure 2. The linear behavior predicted by Eq.15 is readily apparent from the curves shown in Figure 2. Results shown in Table 2 attempt to assess the variation between K_m (from single angle), and K_s (from simulated multiangle) in view of the angular dependence of K_s during coag-flocculation at early time. The agreement between experimental K_m and K_s is satisfactory, indicating correlation between single and multiangle nephelometry.

On a broad base, the discrepancies observed in the results of the functional parameters are due to unattainable assumption that mixing of CWE particles and MSC throughout the dispersion is 100% efficient before aggregation occurs.[20,21] Second account is the interplay between Van der Walls's forces and the hydrodynamic interactions which typically alters the theoretical predicted values by a factor of $\pm$ 2.[21,22]

Time Course % Removal Efficiency of MSC in CWE

Time course removal efficiency (in %) assesses the effectiveness of given dose of MSC in removing SDP from pH varying CWE. Representative results are shown in Figure 3 for 0.15 kg/m^3 MSC dose and varying pH of CWE. The best performance is recorded at pH range of 2–6, with the initial SDP of 138.415 kg/m^3 reduced by 99% at the end of 30 min. Starting from 10 min and above, there was approximately no variation of E(%) with time in respect of pH range of 2–6. With the least recorded E(%) > 90% for all the cases of pH considered, it confirms the effectiveness of MSC to remove turbidity from the CWE at the end of 30 min of coag-flocculation.

Time evolution of cluster-size distribution

Using K_m obtained from Eq. 11, Eq. 13 is able to predict the time evolution of aggregates (monomers, dimmers;

Table 2. Representative Values of K_m (Experimental) and K_s (Simulated) at Varying Dosage and pH

pH	Dosage(kg/m^3)	$(Np)^c_0$(/m^3)	$d_0(\mu m)$	K_m(m^3/kg.s)	K_S(m^3/kg.s)
2	0.15	3.011×10^{26}	0.995	3.333×10^{-3}	3.321×10^{-3}
4	0.15	2.007×10^{27}	0.995	6.667×10^{-3}	6.473×10^{-3}
6	0.15	5.679×10^{25}	0.995	8.333×10^{-3}	7.954×10^{-3}
8	0.15	7.528×10^{26}	0.995	1.667×10^{-3}	1.992×10^{-3}
10	0.15	1.004×10^{28}	0.995	1.167×10^{-4}	1.001×10^{-4}
6	0.05	4.390×10^{25}	0.995	6.666×10^{-3}	6.834×10^{-3}
6	0.10	1.305×10^{27}	0.995	6.666×10^{-3}	7.062×10^{-3}
6	0.15	5.679×10^{25}	0.995	8.333×10^{-3}	8.321×10^{-3}
6	0.2	6.335×10^{25}	0.995	8.333×10^{-3}	8.480×10^{-3}
6	0.25	1.627×10^{26}	0.995	8.333×10^{-3}	8.341×10^{-3}

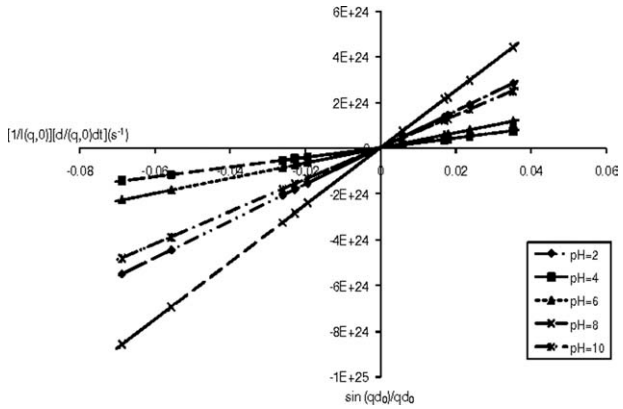

Figure 2. Initial intensity changes vs. interference factor at 0.15 kg/m^3 MSC with varying pH.

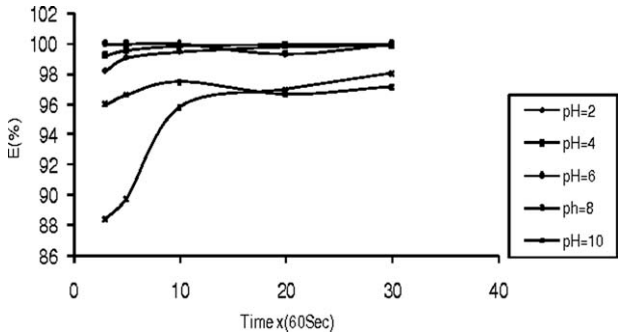

Figure 3. Coag-flocculation efficiency as a function of time.

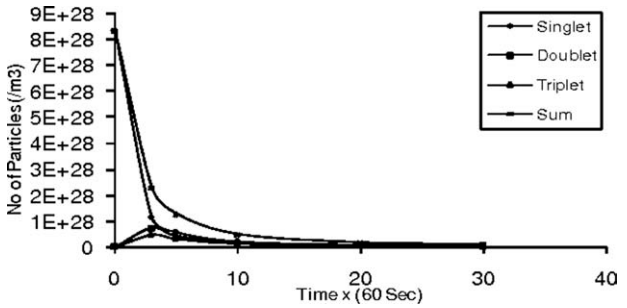

Figure 4. Time evolution of the cluster-size distribution for half-life of 1.7339 s.

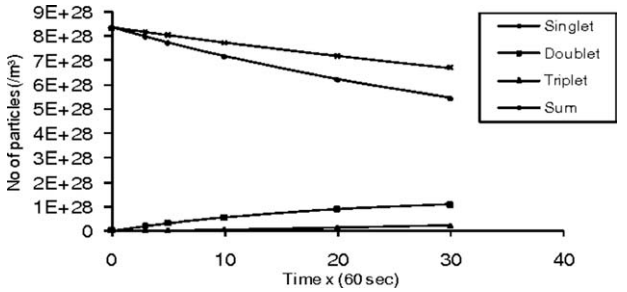

Figure 5. Time evolution of the cluster-size distribution for half-life of 123.854 s.

trimers for $m = 1,2,3$, respectively). Representative results are shown in Figures 4 and 5. The obvious difference in the nature of the curves in response to two different $\tau_{1/2}$ of 1.734 s and 123.854 s are demonstrated as cases 1 and 2, respectively.

Case 1

Consider Figure 4, the primary particles (monomers) and total number of particles can be seen to decrease more rapidly. This is evidence of a high rate of coag-flocculation demonstrated at low $\tau_{1/2}$ of 1.7339 s. This may be explained on the basis of massive and instantaneous destabilization of the particles. With little or no repulsion existing among the particles, the MSC instantly sweeps away the SDP. Arguably, there may be charge reversal such that attraction exists among particle and MSC. This can lead to sweep floc.

Case 2

Figure 5 represents the time evolution of particles at $\tau_{1/2} = 123.854$ s. The curve represents a case in which the values of N_3 and ΣN_i are close such that their variation with time is insignificant. Similar trend is obtained in respect of N_2 and N_1. Figure 5 demonstrates a wide margin of difference in concentration of SDP between the pair of (N_3 and ΣN_i) and (N_2 and N_1). The implication is the existence of high-shear force and resistance to collision, clearly demonstrated by high $\tau_{1/2}$. This is an indication of high-zeta potential associated with the process.

Conclusion

The potentials of MSC as an effective, renewable organic coag-flocculant at a pilot scale have been established. This presents novelty in this work. The establishment of expression $2K_m = \beta_{BR}$ correlating both single and multiangle light scattering theories represents a step further in the advancement of the light scattering studies. The level of agreement between K_m and K_S affirms both single and multiangle light scattering techniques as veritable tools for the routine study of coag-flocculation. The optimum pH and dosage recorded are 6 and 0.15 kg/m3, respectively.

Notation

G = total gibbs free energy, J
D' = diffusion coefficient, m^2/s
K_B = Boltzmanns constant, J/K
T = temperature, K
B = friction factor, Kg/s
$\beta_{BR}(i,j)$ = Brownian aggregation collision factor, m^3/Kg.s
ϵ_p = collision efficiency, Kg^{-1}
η = viscosity of the fluid, Kg/ms
K_R = Von smoluchowski coagulation rate constant, m^3/s
a = particle radius, m
K_m = Menkonu coag-flocculation rate constant, m^3/Kg/s
N_t = concentration of SDP at time t, Kg/m^3
N_0 = initial concentration of SDP, Kg/m^3
$\tau_{1/2}$ = coag-flocculation period, s
$-r$ = coag-flocculation reaction rate, $Kg/m^3.s$
$(Np)_0^c$ = computed initial number of particles/m^3
$(SDP)_0^c$ = computed initial suspended particle, kg/m^3

Literature Cited

1. Ma JJ, Li G, Chen GR, Xu, GO, Cai GQ. Enhanced coagulation of surface waters with high organic content by permanganate per oxidation. *Water Sci Technol Water Supply*. 2001;1(1):51–61.
2. Diterlizzi SD.DiTerlizzi SD. *Introduction to Coagulation and Flocculation of Waste Water*. Environmental Systems Term Project, Fall 1994. Troy, NY: Rensselaer Polytechnic Institute; 1994.
3. Edzwald JK. *Coagulation - sedimentation filtration process for removing organic substances in drinking and waste water*. Park Bridge, NJ: Noyes Data Corp; 1987.
4. O'Meila CR. *Coagulation in waste water treatment*: In:Ives KJ, ed. *The Scientific Basis of Flocculation* (NATO Advanced Study Institute, Series E, Appl. Sci. No 27). Alpenan den Rijn, Netherlands: Sijtholf and Noordhoff; 1978:219–268.
5. Jin Y. Use of High Resolution Photographic Technique for studying Coagulation/Flocculation in Water Treatment [master's thesis]. University of Saskatchewan, Saskatoon, Canada; 2005:22–29.
6. Guerranti R, Aguiyi JC, Neri S, Leoncini R, Pagani R, Marinello E. Proteins from *mucuna pruriens* and enzymes from *echis carrinatus* venom. *J Biol Chem.* 2002;10;277(19):17072–8. DOI 10.1074/jbc.M201387200.7.
7. Echendu CA. Nutritional value of processed and raw food thickeners commonly used in south eastern Nigeria. *Afr J Sci*. 2004;5(1):1107–1121.
8. Hunter RJ. *Introduction to Modern Colloid Science*. 4th ed. New York: Oxford University Press; 1993:33–38;289–290.
9. Thomas DN, Judd SJ, Fawcett N. Flocculation modeling: A review. *Water Res*. 1999;33(7):1579–1592.9.
10. Swift, DL, Friedlander S.K. The coagulation of hydrolysis by Brownian motion and laminar shear flow. *J Colloid Sci*. 1964;19:621.
11. Fridkhsberg DA. *A Course in Colloid Chemistry*. Moscow, Russia: Mir Publishers; 1984:266–268.
12. Van Zanten, JH, Elimelech M. Determination of Rate constants by multi angle light scattering. *J Colloid Interface*. 1992:154(1);621.
13. Water Specialist Technology (WST). About Coagulation and Flocculation: Information Bulletins; 2003.
14. Menkiti MC. Studies on the Rapid Coagulation and Flocculation of Coal Washery Effluent: A Turbidimetric Approach [MS Thesis]. Dept. of Chemical Engineering, Nnamdi Azikiwe University, Awka, Nigeria; 2007.
15. Menkiti MC, Igbokwe PK, Ugodulunwa FXO, Onukwuli OD. Rapid coagulation/flocculation kinetics of coal effluent with high organic content using blended and unblended chitin derived coagulant (CDC). *Res J Appl Sci*. 2008;3(4):317–323.
16. Menkiti MC, Nnaji, PC, Onukwuli OD. Coag-flocculation kinetics and functional parameters response of periwinkle shell coagulant (PSC) to pH variation in organic rich coal effluent medium. *Nature Sci*. 2009;7(6):1–18.
17. Menkiti MC, Nnaji PC, Nwoye CI, Onukwuli OD. Coag-flocculation kinetics and functional parameters response of mucuna seed coagulant to pH variation in organic rich coal effluent medium. *J Mineral Mater Character Eng*. 2010;9(2):89–103.
18. Adebowale YA, Adebowale KA. Evaluation of the gelation characteristics of mucuna bean flour and protein isolate. *Electron J Environ Agric Food Chem*. 2007;6(8):2243–2262.
19. AWWA. *American Water Works Association*. In: *Standard Methods for the Examination of Water and Waste Water Effluent*, 16th ed. New York, NY: American Public Health Association (APHA); 1985.
20. Yates P, Yan Y, Jamson GJ, Biggs S. Heteroaggregation of Particle System: Aggregation Mechanisms and Aggregate Structure Determination, 6th World Congress of Chemical Engineering, Melbourne, Australia, 23rd -27th September 2001. 2001:1–10.
21. Holthof H, Schmitt A, Fernández-Barbero, Borkovec M, Cabrerizo-Vilehez, Schurtenberger P, Hidalgo-Alvarez R. Measurement of absolute coagulation rate constants for colloidal particles: comparison of single and multi angle light scattering techniques. *J Colloid Interface Sci*. 1997;192:463–470.
22. Holthof H, Egelhaaf SU, Borkovec M, Schurtenberger P, Sticher H. Coagulation rate measurement of colloidal particles by simultaneous static and dynamic light scattering. *Langmuir*. 1996;12:5541.

Manuscript received June 16, 2009, and revision received Mar. 17, 2011.